

Dynamics of Electron-Rich Plasmas in the CNT Stellarator

Thomas S. PEDERSEN, John W. BERKERY, Allen H. BOOZER, Paul W. BRENNER, Benoit Durand de GEVIGNEY, Michael S. HAHN, Quinn R. MARKSTEINER and Haruhiko HIMURA¹⁾

Columbia University, New York, NY 10027, USA

¹⁾*Kyoto Institute of Technology, Matsugasaki, Kyoto 606-8585, Japan*

(Received 28 November 2007 / Accepted 5 February 2008)

Pure electron plasmas and electron plasmas with a finite ion fraction have been studied in the Columbia Non-neutral Torus (CNT) since the end of 2004. Results from the first three years of operation are summarized. Stable, small Debye length pure electron plasmas are routinely created, and have confinement times up to 20 msec. The confinement is limited by radial transport caused by internal rods, as well as electron-neutral collisions. The neutral driven transport rate is indicative of poor particle orbits in CNT, despite the strong radial electric field. Numerical simulations shed light on this issue, demonstrating the detrimental effects of variations in the electrostatic potential on a magnetic surface. With the installation of a magnetic surface conforming electrostatic boundary and the transition to external diagnostics, significantly longer confinement times should be possible. Also presented are observations of sudden confinement jumps that have a hysteretic behavior, and observations of an ion driven instability.

© 2008 The Japan Society of Plasma Science and Nuclear Fusion Research

Keywords: stellarator, non-neutral plasmas, neoclassical confinement, magnetic surfaces

DOI: 10.1585/pfr.3.S1022

1. Introduction

The Columbia Non-neutral Torus (CNT) is a modest scale stellarator dedicated to the studies of non-neutral and electron-positron plasmas confined on magnetic surfaces. CNT is the lowest aspect ratio stellarator constructed to date, $A < 1.9$, and is unique in the simplicity of the coil configuration. The CNT stellarator has only four circular coils, Fig. 1. Details of the CNT design and construction can be found in References [1, 2]. CNT was assembled rather easily primarily by graduate students, an advantage of the error field resilience in the design. The quality of the magnetic surfaces was confirmed by electron-beam magnetic surface mapping [3].

The physics of non-neutral plasmas on magnetic surfaces is of interest because the magnetic surface topology allows pure electron plasmas to reside in an equilibrium that is a minimum energy state [4, 5] rather than a maximum energy equilibrium as is the case for pure electron plasmas in Penning traps and pure toroidal field traps [6, 7]. The physics of these non-neutral plasmas in CNT is also of interest in terms of neoclassical stellarator transport in the presence of strong radial electric fields. The non-neutral plasmas in CNT allow exploration of neoclassical transport in the limit $|e\phi_p|/T_e \gg 1$. This is the limit where the $E \times B$ drift is dominant and is predicted to yield excellent confinement even for a classical stellarator such as CNT [4, 8]. Because of the electron space charge, CNT has a very strong, negative electric field. It is in an extreme version of the so-called ion root of stellarator neoclassical

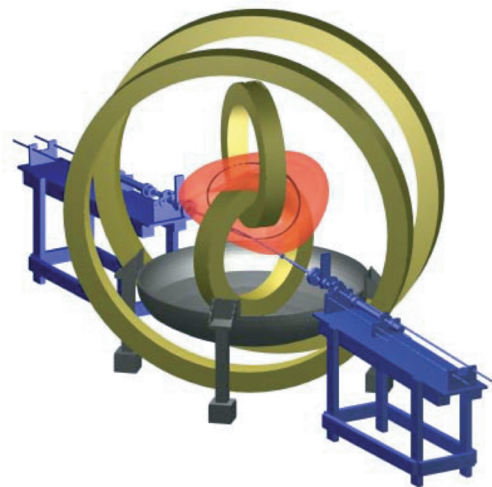


Fig. 1 A CAD drawing showing the CNT design, including the four circular coils, the magnetic surface shape, and the locations of probe rods.

transport. CNT's electric field is externally controlled and does not need to satisfy ambipolarity. This is the reason that CNT can access the regime $|e\phi_p|/T_e \gg 1$ which is not accessible in quasi-neutral plasmas.

2. Creation and Diagnosis of Pure Electron Plasmas in CNT

Pure electron plasmas are created in CNT by thermionic emission from heated filaments placed inside

author's e-mail: tsp22@columbia.edu



Fig. 2 A picture of the hot emissive filaments mounted on ceramic rods inserted into the magnetic surfaces of CNT.

the magnetic surfaces, Fig. 2. The filaments are biased negatively relative to the vacuum chamber and internal coils. Typically only one filament is used to maintain the plasma density, and the others are used as probes, measuring plasma potential, density, and temperature [9]. The emission rate is typically in the μA range, indicating good confinement and a close match between the local plasma potential and the filament bias potential. This close match is confirmed by independent measurements of the plasma potential. Hence, the bias potential sets the central plasma potential ϕ_p , which is linearly related to the total electron inventory through Poisson's equation. CNT plasmas are created and maintained for minutes, sometimes hours at a time, in a complete steady state. This implies that the electron emission rate from the biased filaments equals the radial loss rate of electrons. The ion content is also in steady state, the ion density being determined by the balance between volumetric ionization of neutrals and recombination of ions as they strike the internal rods [10].

3. Equilibrium Properties

A typical operating point for CNT is $B = 0.02$ T, $p_n = 1 \times 10^{-8}$ Torr, $\phi_p = -200$ V. This yields $n_e \approx 10^{12}$ m $^{-3}$, $T_e = 4$ eV, $\lambda_D = 1.5$ cm, and $n_i/n_e < 1\%$. Radial profiles of T_e , n_e , and ϕ_p are measured and are used as inputs for the numerical reconstructions of CNT equilibria in three dimensions [11, 12]. The equilibrium equation for a pure electron plasma on magnetic surfaces is given by [4]:

$$\epsilon_0 \nabla^2 \phi = eN(\psi) \exp\{e\phi/T_e(\psi)\}. \quad (1)$$

Here, ψ is a magnetic surface coordinate (a minor radial coordinate in a simple circular cross section tokamak-like configuration). Eq. 1 is Poisson's equation with the space charge coming from electrons in a Boltzmann distribution on each magnetic surface, $n_e = N(\psi) \exp\{e\phi/T_e(\psi)\}$. As indicated, T_e is assumed constant on each magnetic surface due to rapid parallel temperature equilibration. This equation is solved numerically in the CNT geometry. The equi-

libria have some interesting, non-trivial properties. For example, the equilibria are quite sensitive to the electrostatic boundary condition, even when the Debye length is relatively short, as is the case for the plasmas studied in CNT $\lambda_D = 1.5$ cm $\ll a \approx 15$ cm. This comes about because of the peculiar nature of Debye screening in a non-neutral plasma. If a pure electron plasma is subjected to a perturbation $\delta\phi_{\text{ext}}$ to its equilibrium potential, the situation will be rather different depending on the strength of the perturbation. If $|e\delta\phi_{\text{ext}}/T_e \ll 1$, the expected Debye screening will occur even in a pure electron plasma [13]. However, if $-e\delta\phi_{\text{ext}}/T_e \gg 1$, the electron density $n_e \propto \exp(e\phi/T_e)$ will be severely depleted from the region around this perturbation. Without ions, this ends up being essentially a vacuum region so there is little Debye screening. Thus, by evacuating parts of the magnetic surface of electrons, the external electrostatic boundary condition may affect the plasma several Debye lengths inside the last closed flux surface. This effect has been seen in the numerical equilibrium reconstructions for CNT and affects the transport in CNT, as discussed in Section 4.

Large density variations along the magnetic field are not only predicted as a consequence of the external electrostatic boundary, but are also intrinsic to CNT equilibria, occurring even on the magnetic axis and at a magnitude that is largely independent of the electrostatic boundary condition for small Debye length plasmas. This is due to the combination of the electrostatic equilibrium and the strongly varying cross sectional shape of the CNT magnetic surfaces. This was discovered numerically [14] and has recently been confirmed experimentally [15].

4. Understanding and Improving Confinement

Experimentally, it was quickly established that the insulated rods holding the emissive filaments were driving transport, in fact dominating transport at low neutral pressures, $p_n < 2 \times 10^{-8}$ Torr [11]. Neutral driven electron transport is also observed, and even though the two transport mechanisms currently coexist in CNT, they can be studied separately by varying the neutral pressure. The rod driven transport is due to the electrostatic perturbation that the rods create. Since the rods are insulating, they are not steady state sinks for the electron plasma, but charge up negatively to self-shield against the electrons in the plasma. The electric field around the rod that pushes electrons away from the rod also creates an $E \times B$ drift across the magnetic surfaces (radially) and allows electrons to escape. The observed rod-driven transport is in good agreement with a model of this process [16].

The neutral driven transport scales linearly with neutral pressure, as one would naively expect, but is much faster than expected. Experiments show that an electron is lost after approximately one collision with a neutral [16]. Such rapid loss usually implies that there is a large loss

cone, that is, there are many unconfined particle orbits in CNT. CNT is a classical stellarator with substantial ripple, and has a large fraction of trapped particles, $> 50\%$. Nonetheless, the particle confinement in CNT is expected to be many collision times [8] due to the strong $E \times B$ drift which forces the trapped particles to precess poloidally. This apparent inconsistency is now being resolved by a numerical investigation of particle orbits in CNT. These numerical simulations show that the mismatch between the electrostatic potential surfaces ($\phi_p = \text{constant}$) and the magnetic surfaces allows a large fraction of the electrons in CNT to move radially from the core region to the open magnetic surfaces, at which time they are lost. Intuitively, this process can be understood as follows. In the absence of an electrostatic potential, and ignoring magnetic drifts for the sake of simplicity, passing particles circulate around on the magnetic surfaces, poloidally and toroidally. When there is an electrostatic potential present, the $E \times B$ drift allows the electrons to move on the electrostatic potential surfaces. If these surfaces do not coincide with the magnetic surfaces, the electron can move to an outer magnetic surface, then move along the magnetic surface (by parallel motion, possibly being accelerated by a small parallel electric field). On this other part of the magnetic surface, it may drift along another electrostatic contour out to a magnetic surface farther out. This pattern may repeat itself enough that the particle finds its way outside the last closed flux surface, without the need for any collisions. These unconfined orbits have been observed in our numerical simulations, and are currently being investigated and will be described fully in an upcoming publication. If one enforces an electrostatic potential that is constant on the magnetic surface in these simulations, the loss orbits disappear and excellent confinement is predicted. It should be noted that a quasineutral plasma will enforce a constant electrostatic potential almost exactly, so this loss mechanism is likely negligible in quasi-neutral stellarator plasmas. This loss mechanism, together with the aforementioned sensitivity to external potential variations even in a small Debye length pure electron plasma, implies that the electrostatic boundary condition is very important for confinement in CNT.

Until the summer of 2007, and for all the experimental data described here, the electrostatic boundary condition for the CNT plasmas was set by the grounded internal coils as well as the grounded vacuum chamber. This is an electrostatic boundary condition that does not conform to the magnetic surfaces. Therefore it contributes significantly to electrostatic potential variations on the magnetic surfaces, and radial transport. A segmented copper mesh conforming to the shape of the magnetic surfaces has recently been installed in CNT, Fig. 3. Once it is aligned properly to the magnetic surfaces, it is expected to vastly improve confinement in CNT. It will also be used as a capacitive (image charge) electrostatic probe external to the plasma. This combined with a recently installed retractable



Fig. 3 The copper mesh electrostatic boundary installed in the CNT experiment.

emitter [17] will eliminate the need for internal probes and will hopefully improve confinement in CNT substantially.

5. Confinement Jumps

Under experimental conditions that favor very large radial electron fluxes (i.e., large emission currents from the biased filament), sudden jumps in the emission current are seen as parameters controlling the emission current are varied. These emission current jumps display hysteretic behavior and they can be as large as a factor of two. Figure 4 shows results from experiments where the emission current is varied by scanning the bias potential on the emitter, and therefore, the central plasma potential. The large abrupt jumps and the hysteretic behavior are clearly seen. Experiments are performed over long enough time scales (typically tens of seconds) that the plasmas are all in steady state and the emission current equals the radial loss rate of electrons. Thus, the jumps in emission current are also jumps in transport. These jumps occur at particular transport rates whether the transport is changed by varying the emitter bias, magnetic field strength, plasma potential, neutral pressure, or the number of insulating rods in the plasma. The jumps do not occur in the parameter range described earlier, rather they occur when transport is significantly enhanced, i.e., confinement is reduced, relative to the normal operating range.

Taking advantage of the hysteretic behavior, the experimenter can choose either the poorly confined (high emission current) state, or the well confined state, by approaching a particular bias potential either from above or below. This allows one to investigate the two equilib-

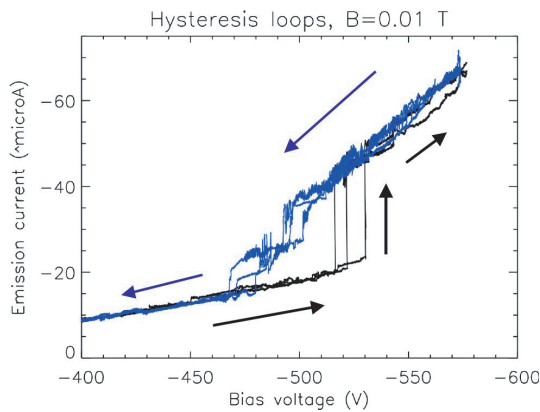


Fig. 4 Several confinement jumps for the same nominal plasma conditions, showing the hysteretic behavior, and indicating the degree of reproducibility of the jumps. The arrows and the colors indicate the time history (black indicates traces where the potential is increasing over time, blue indicates traces where the potential is decreasing over time).

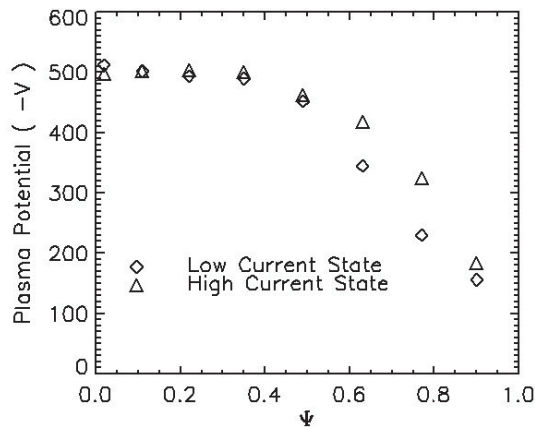


Fig. 5 The potential profile measured at the same emitter bias in the two equilibrium states of the confinement jump.

ria associated with the large and the small radial electron transport, at the same central plasma potential. It is found that the two states of transport are associated with different equilibrium states of the plasma. This is evidenced by the distinctly different radial plasma potential profiles in the two states (Fig. 5). Numerical reconstructions of these two equilibrium states have been performed [12]. These determine the electron inventory, for each state, which allows the calculation of the confinement time. The abrupt positive transport jumps correspond to abrupt drops in the confinement time.

When varying the central plasma potential, the electron inventory is clearly varied also. The transport rate of the plasma may be increased in several other ways that do not change the zero order electron inventory and the jumps are still observed at the same transport rates.

In low temperature quasineutral plasmas, hysteretic current jumps are also observed under some conditions.

These jumps are believed to be associated with ionization of neutrals [18, 19]. By contrast, ionization does not play a role in the hysteretic jumps in CNT. The jumps are observed at a variety of neutral pressures, including ones that are so low that the ion content is negligible, $n_i/n_e < 1\%$. In addition, the ion content in CNT is reduced by a factor of two when the number of internal rods is doubled. The transport jumps occur at the same emission current levels under these conditions, conclusive evidence that the jumps are not associated with ionization.

The transport jumps are currently under investigation in CNT and will be discussed in greater detail in a future publication.

6. Ion Resonant Instabilities

By increasing the neutral pressure well above the base pressure of CNT (which is $p_n \approx 5 \times 10^{-9}$ Torr), electron-rich plasmas with a significant ion fraction can be studied. When the ion fraction exceeds approximately 10% of the electron density, an oscillation is observed [20].

Fig. 6 shows the onset of this oscillation, as detected on an internal floating emissive probe, as the neutral pressure of hydrogen gas (H_2) is increased. As seen in Fig. 7, the oscillation frequency decreases with increasing magnetic field, but does not depend on the ion fraction, which was controlled by the neutral pressure in these experiments. Fig. 8 shows that the frequency of the instability increases approximately linearly with ϕ_p . These frequency trends suggest a link to the $E \times B$ flow of the plasma. However, the frequency does not scale exactly as $1/B$. It starts deviating significantly from a $1/B$ scaling at low magnetic field strengths (< 0.04 Tesla). Also, the observed frequency depends on the ion species used to drive the plasma unstable, with slightly higher frequency for lighter ions [20], whereas the $E \times B$ frequency is independent of ion species.

The fact that the frequency of the instability is independent of ion density indicates that it is not a simple plasma sheath-emissive probe instability, which would have a frequency that is proportional to the ion plasma frequency, $\omega_{pi} \propto \sqrt{n_i}$. The frequency does not scale exactly as $1/B$, and depends on the ion species introduced, so the instability is not a pure-electron mode that is driven by the presence of ions; as is the case for the ion driven instability observed in Penning traps [21, 22]. There is a stronger measured frequency dependence of the instability at low B than the frequency dependence of the ions by themselves [20], implying that the instability involves both a perturbed electron and ion component.

It is therefore concluded that the instability involves a resonant interaction between the ions and electrons. The observed frequency of the instability is in the range of orbital frequencies of the ions, which are marginally magnetized at low magnetic field strengths, and the electron $E \times B$ frequency.

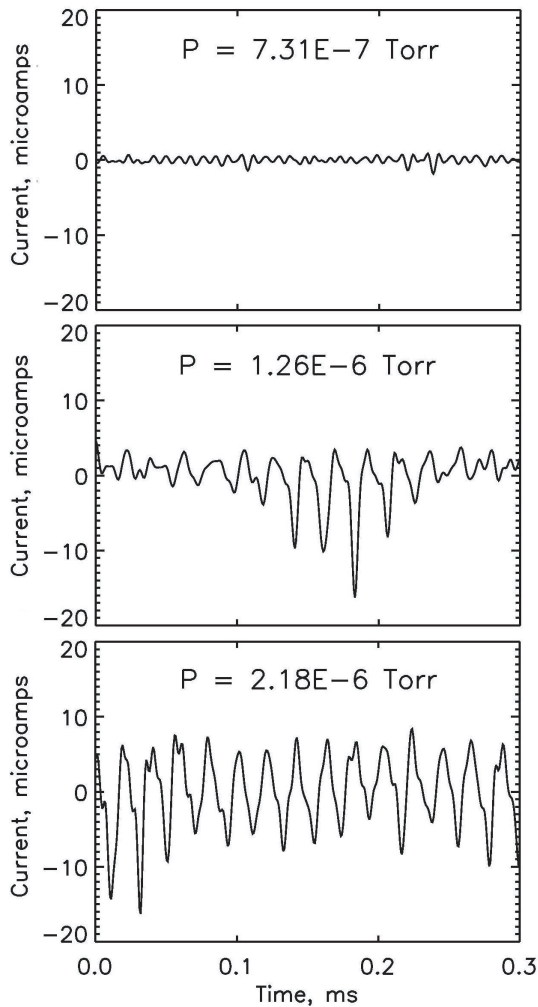


Fig. 6 Measurements of the electron current of a floating emissive probe show the onset of the instability as the neutral pressure is raised. In this case, the neutral gas was H_2 .

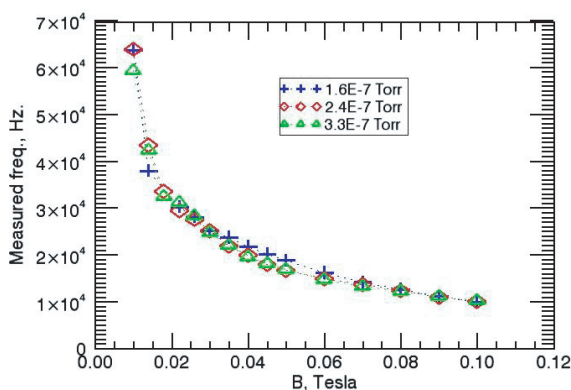


Fig. 7 The frequency of the instability vs. magnetic field strength, at three different neutral pressures of N_2 . Here $\phi_p = -200$ Volts.

The instability has a poloidal mode number $m = 1$, which is not resonant with any of the magnetic surfaces in CNT [20]. It is interesting to note that $m = 1$ is also the

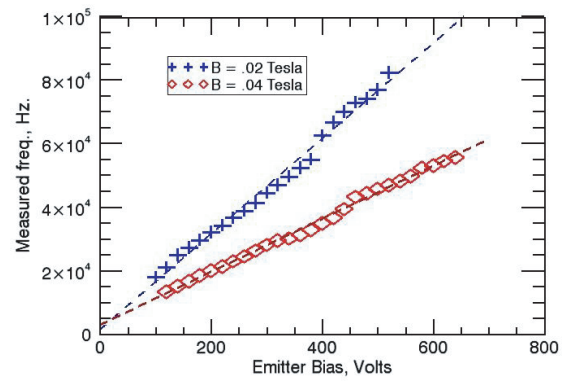


Fig. 8 The frequency of the instability vs. ϕ_{plasma} , at two different magnetic field strengths. The background neutral pressure is 2.5×10^{-7} Torr of N_2 .

poloidal mode number observed in Penning traps [22] and pure toroidal field traps [23, 24]. However, in these traps, parallel force balance is not violated, as they do not have magnetic surfaces or any rotational transform. The numerical simulations of electron motion in CNT, described in Section 4, show that $\approx 65\%$ of electrons are on trapped orbits in CNT. It may be that the violation of electron parallel force balance that is present when the plasma is unstable can occur because of the large fraction of trapped electrons.

Acknowledgments

This work is supported by the NSF CAREER program, Grant No. NSF-PHY-04-49813, the NSF-DOE Partnership in Plasma Science, Grant No. NSF-PHY-06-13662, and the Fusion Energy Sciences Postdoctoral Research Program of the US Department of Energy.

- [1] T. Sunn Pedersen, A.H. Boozer, J.P. Kremer, R.G. Lefrancois, F. Dahlgren, N. Pomphrey and W. Reiersen, *Fusion Sci. Technol.* **46**, 200 (2004).
- [2] T. Sunn Pedersen, J.P. Kremer, R.G. Lefrancois, Q. Marksteiner, N. Pomphrey, W. Reiersen, F. Dahlgren and X. Sarasola, *Fusion Sci. Technol.* **50**, 372 (2006).
- [3] T. Sunn Pedersen, J.P. Kremer, R.G. Lefrancois, Q. Marksteiner, X. Sarasola and N. Ahmad, *Phys. Plasmas* **13**, 012502 (2006).
- [4] T. Sunn Pedersen and A.H. Boozer, *Phys. Rev. Lett.* **88**, 205002 (2002).
- [5] A.H. Boozer, *Phys. Plasmas* **11**, 4709 (2004).
- [6] J. Notte, A.J. Peurrung and J. Fajans, *Phys. Rev. Lett.* **69**, 3056 (1992).
- [7] T.M. O'Neil and R.A. Smith, *Phys. Plasmas* **1**, 2430 (1994).
- [8] J.W. Berkery and A.H. Boozer, *Phys. Plasmas* **14**, 104530 (2007).
- [9] J.P. Kremer, T. Sunn Pedersen, Q. Marksteiner, R.G. Lefrancois and M. Hahn, *Rev. Sci. Instrum.* **78**, 013503 (2007).
- [10] J.W. Berkery, Q. Marksteiner, T. Sunn Pedersen, J.P. Kremer, *Phys. Plasmas* **14**, 084505 (2007).

- [11] J.P. Kremer, T. Sunn Pedersen, R.G. Lefrancois and Q. Marksteiner, Phys. Rev. Lett. **97**, 095003 (2006).
- [12] R.G. Lefrancois, T. Sunn Pedersen, A. H. Boozer and J. P. Kremer, Phys. Plasmas **12**, 072105 (2005).
- [13] R.C. Davidson, "*Physics of Nonneutral Plasmas*", (World Scientific, 2001) p.59-61.
- [14] R.G. Lefrancois and T. Sunn Pedersen, Phys. Plasmas **13**, 120702 (2006).
- [15] M.S. Hahn, T. Sunn Pedersen, Q. Marksteiner and J. W. Berkery, submitted to Phys. Plasmas, (2007).
- [16] J.W. Berkery, T. Sunn Pedersen, J.P. Kremer, Q.R. Marksteiner, R.G. Lefrancois, M.S. Hahn and P. W. Brenner, Phys. Plasmas **14**, 062503 (2007).
- [17] J.W. Berkery, T. Sunn Pedersen and L. Sampedro, Rev. Sci. Instrum. **78**, 013504 (2007).
- [18] R.A. Bosch and R.L. Merlino, Contrib. Plasma Phys. **26**, 1 (1986).
- [19] R. Timm and A. Piel, Contrib. Plasma Phys. **32**, 599 (1992).
- [20] Q.R. Marksteiner, T. Sunn Pedersen, J.W. Berkery, M.S. Hahn, J.M. Mendez, B. Durand de Gevigney and H. Himura accepted in Phys. Rev. Lett. (2008).
- [21] J. Fajans, Phys. Fluids B **5**, 3127 (1993).
- [22] A.J. Peurrung, J. Notte and J. Fajans, Phys. Rev. Lett. **70**, 295 (1993).
- [23] M.R. Stoneking, M.A. Growdon, M.L. Milne and R.T. Peterson, Phys. Rev. Lett. **92**, 095003 (2004).
- [24] J.D. Daugherty, J.E. Eninger and G.S. Janes, Phys. Fluids **12**, 2677 (1969).